

How to measure the volume fraction of granular assemblies using x-ray radiography

Manuel Baur^{a,*}, Joelle Claussen^c, Stefan Gerth^c, Jonathan Kollmer^d, Tara Shreve^{b,a}, Norman Uhlmann^c, Thorsten Pöschel^a

^a*Lehrstuhl für Multiscale Simulation, Friedrich-Alexander-Universität Erlangen-Nürnberg, Nägelsbachstraße 49b, 91052 Erlangen, Germany*

^b*Institut de Physique du Globe, 1 Rue Jussieu, Paris 75005, France*

^c*Fraunhofer Development Center X-Ray Technology (EZRT), Fraunhofer-Institut for Integrated Circuits IIS, Flugplatzstraße 75, 90768 Fürth, Germany*

^d*Department of Physics, North Carolina State University, Raleigh, North Carolina 27695, USA*

Abstract

When investigating dynamical processes in granular systems, it is frequently necessary to measure the time-resolved local material density. Recently, x-ray radiography facilities became available in many laboratories and can be used to measure the volume fraction via the attenuation of x-ray radiation along the beam direction. Naïve application of the Beer-Lambert law yields, however, unacceptably large systematic errors due to beam hardening. We present a calibration protocol which allows to reliably measure the local volume fraction based exclusively on reference measurement of known packing fraction.

Keywords: volume fraction, x-ray radiography, beam hardening

1. Introduction

In many cases, the dynamics of granular matter depend sensitively on the local volume fraction of the system. A prominent example is the formation of shear bands which requires local reduction of density due to Reynolds dilatancy. Reliable measurements of volume density are necessary for the quantitative investigation of many granular systems such as irregular granular pipe and hopper flow, fluidized beds, multi-phase flows, etc. which are essential for many industrial applications. In some cases, such as dense shear flows, the dynamical properties vary drastically due to short term variations of the local volume density, resulting in a demand for reliable and precise measurements. The attenuation of x-ray radiation allows to measure the material density. Nowadays x-ray setups are available as standard devices in many laboratories. Due to the progress of modern flat panel detectors large frame rates with high signal-to-noise ratio can be reached. This allows the study of dynamic granular systems using x-ray radiography. The naïve application of Beer-Lambert's law will, however, lead to inaccurate measurements due to beam hardening.

In this *short communication*, we propose a protocol for calibration of x-ray radiography measurements which relies exclusively on reference measurement of a sample of known volume fraction. We exemplify the method for the case of shear bands in a horizontally vibrated granular system and obtain a correction for the packing density. Naïve

measurements, where no correction with respect to beam hardening is applied, lead to large systematic errors.

2. Measurement of volume fraction and errors due to beam hardening

When monochromatic x-rays penetrate matter, the incident intensity, I_0 , emitted from the source is attenuated exponentially,

$$I = I_0 e^{-\mu \Delta x}, \quad (1)$$

known as *Beer-Lambert law* (Beer, 1852), where Δx is the thickness of the material, and μ its specific attenuation coefficient. In the grain material, the intensity of the beam decreases due to Rayleigh scattering, photoelectric absorption, and Compton scattering by the electrons of the material. For photon energies above $2m_e c^2 = 1.022$ MeV, electron-positron pair production also occurs. All these contributions to the attenuation coefficient depend on the photon energy E . Furthermore, the attenuation depends on the number of electrons, which is given by the atomic number Z of the grain material. In the case of a polychromatic broad x-ray spectrum $\omega(E)$ equation 1 must be extended to

$$I = I_0 \int_0^{E_{\max}} \omega(E) \exp\left(-\int_0^{l_{\max}} \mu(E, l) dl\right) dE. \quad (2)$$

The attenuation coefficient is a function of the photon energy E and the path length l of the beam inside the material of width l_{\max} . To describe the attenuation of the whole spectrum $\omega(E)$ an effective attenuation coefficient

*Corresponding author

Email address: manuel.baur@fau.de (Manuel Baur)

can be introduced Kleinschmidt (1999). Subsequently the term attenuation is used that way.

The dependence on l allows to distinguish the internal structure of objects, even if from outside no structure is noticeable. The attenuation can be also used to measure the density of a granular system, which is connected to the path length of the beam in the grains, see Fig. 1: Beam (a) arrives at the detector with an intensity I_0 due

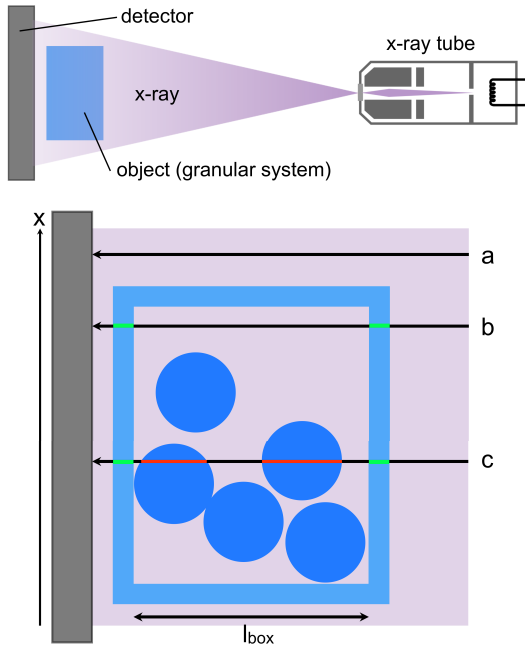


Figure 1: Sketch of the experiment (top). Note that the distance between the x-ray lamp and the object was scaled down. The cone beam geometry (top) is approximated by a parallel beam, shown in the magnification (bottom). Beam (a) is negligibly attenuated by the ambient air, while beams (b) and (c) are attenuated by the container material and the granulate, respectively. The intervals which contribute to the attenuation are highlighted by green and red color. The detector is in the (x, y) plane, where x is shown and y is perpendicular to the paper plane.

to the fact that the attenuation by the ambient air can be neglected with respect to the attenuation of solid matter. Beam (b) is attenuated by passing only the container walls (discussed below) and beam (c) by passing the container walls and the granular material. Hereby, only the spacial intervals occupied by grain material contributes to the attenuation; the corresponding intervals of the beam's path are highlighted by red color in Fig. 1. Thus, by measuring the intensity of the attenuated beam at a certain position (x, y) of the detector, we can determine the total path length, $l_g(x, y)$, along this beam which is occupied by grains. The local density is then determined by

$$\langle \varphi \rangle = \frac{l_g(x, y)}{l_{\text{box}}}, \quad (3)$$

where l_{box} is the inner length of the box in the beam direction. The average volume fraction is then obtained by

averaging the local density,

$$\langle \varphi \rangle = \frac{1}{A} \iint \varphi(x, y) dx dy, \quad (4)$$

where A is the area of the box in the xy -plane. Combining Eqs. (1) and (3), where $\Delta x = l_g$, allows to identify variations of density in granular systems by means of x-ray radiograms. The fact that the x-ray beam is strongly attenuated in dense regions, compared to dilute regions, has been applied, e.g., to study density waves in flowing sand Michalowski (1984); Baxter et al. (1989), dilatancy due to slow shear Kabla and Senden (2009), and the formation of a granular jet after a sphere impacts into a loose granular packing Royer et al. (2005); Homan et al. (2015).

When it comes to *quantitative* measurements of granular densities beyond gray-scale imaging, however, we are faced with a problem: from the above mentioned energy dependent interaction probability of x-ray photons with the electrons of the grain material, we see immediately that the Beer Lambert law, Eq. (1), is valid only for monochromatic x-rays where all photons have the same energy, E . Common x-ray tubes generate, however, polychromatic x-rays, thus, the spectral composition of the x-rays alters as a function of the penetration length, Δx , through the material. More specifically, the low-energy (long wavelength) photons undergo scattering and absorption events at a higher probability than high-energy photons with the consequence that the spectrum of the x-ray beam shifts to high-energy, also called *hard radiation*. This effect is, therefore, referred to as *beam hardening*. In many applications, x-ray radiography is used to identify structural features from images. Here, beam hardening may be tolerable or even exploited to enhance contrast. For quantitative investigations, however, beam hardening is critical as it results in erroneous information about the sample's composition and density.

A simple solution would be to calibrate the detector at different volume fractions $\phi(x, y)$ to deliver the correct value of $l_g(x, y)$ from a measured intensity, $I(x, y)$, irrespective of beam hardening and other sources of error. The problem here is that there is no simple way to produce a granular system at all values of densities which are of interest for the measurement, in order to calibrate our device.

3. Analyzing x-ray radiograms

In order to determine $\varphi(x, y)$ from Eqs. (1) and (3), we need to take two effects into account: beam hardening and the extinction due to the container walls. Beam hardening implies that the attenuation coefficient of the granular material μ_g is a function of l_g . The actual functional form depends on the details of the x-ray generation (target material, acceleration voltage) and on the energy resolved sensitivity of the detector. While there is no closed theory for the derivation of $\mu_g(l_g)$, an empirical expression

proposed by Yu et al. (1997) will be used here as an approximation to interpolate experimental data:

$$\mu_g(l_g) = \frac{\mu_0}{1 + \lambda l_g}, \quad (5)$$

with open parameters μ_0 and λ . Therefore, we obtain Lambert Beer's law in the form

$$I = I_0 e^{-\mu_g(l_g)l_g} e^{-\mu_w(l_w)l_w} = I_0 e^{-\mu_g(l_g)l_g - M}, \quad (6)$$

where μ_w is the attenuation coefficient of the wall material and l_w is the path length through the sidewalls. In our case, sketched in Fig. 1, the wall thickness is independent of (x, y) , therefore, we can introduce the constant M to characterize the attenuation due to the container walls. Its value can be determined from a single measurement of the empty container (beam (b) in Fig. 1):

$$M = \mu_w(l_w)l_w = -\ln \frac{I^{(b)}}{I_0} \quad (7)$$

where $I^{(b)}$ is the intensity of beam (b), and I_0 can be measured in an area of the radiogram which is outside of the object (beam (a) in Fig. 1),

$$I_0 = I^{(a)}. \quad (8)$$

Knowing M and I_0 , as well as Eq. (7) and (8), from Eqs. (5) and (6) we obtain l_g . Keeping in mind that l_g is a function of the position (x, y) at the detector, we obtain

$$l_g(x, y) = \frac{1 + \lambda l_g(x, y)}{\mu_0} \left(\ln \frac{I(x, y)}{I_0} - M \right). \quad (9)$$

With Eq. (3) we get,

$$\varphi(x, y) = \frac{1}{l_{\text{box}} \mu_0 + \lambda \ln \frac{I(x, y)}{I_0} + \lambda M} \left(-\ln \frac{I(x, y)}{I_0} - M \right), \quad (10)$$

which allows to determine the density field, $\varphi(x, y)$, from the measured field of intensities, $I(x, y)$. Equation (10) contains the yet unknown parameters μ_0 and λ which can be determined by a fit to a calibration measurements. Usually a wedge is used to map the gray value to an X-ray penetration length. A wedge is geometrically not symmetric relative to the X-ray beam. Here we used a rectangular shaped box to avoid the resulting asymmetric scattering inside the wedge. This box is filled with the same granulate as used for the actual measurements, which is sand in our case. The homogeneity of the sand packing can be verified by an even gray value. This crosscheck of the packing can not be performed with a wedge shaped box. Three calibration measurements are done by rotating the rectangular container by 90 degrees relative to the beam.

4. Example

We consider an horizontally vibrated container (amplitude 18 mm, frequency 18 Hz) partially filled by granular

material such that the upper part of the granulate sloshes back and forth, see Fig. 2. A full size paper on this experiment including all details of the experiment will be published elsewhere (Kollmer et al., 2018). The system develops recurrent shear bands which give rise to a complicated spatio-temporal phenomenology (Pöschel and Rosenkranz, 1998; Pöschel et al., 2012). X-ray radiography with the cal-

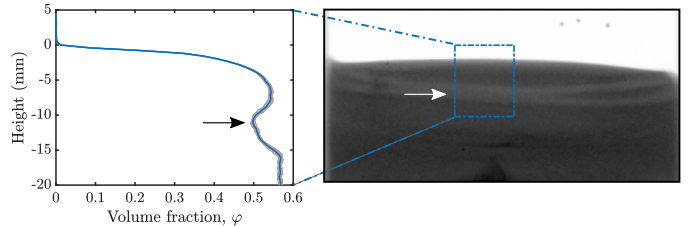


Figure 2: Right: X-ray radiogram of a horizontally vibrated container partially filled with granular material. Due to the vibration, the upper part of the material sloshes back and forth giving rise to a shear band pattern. Left: Volume fraction as a function of height, averaged horizontally over the central region of the radiogram indicated by the marked box. The gray shadow of the blue curve represents the standard deviation of φ in horizontal direction within the area of the marked area. The arrows indicate the vertical position of the shear band.

ibration protocol described above allows to quantitatively measure the volume fraction of the granular system as a function of space and time. The shear band structure is not stationary but oscillates at a frequency of ca. 0.5 Hz which makes it difficult to investigate this system using other methods. The container was made from polycarbonate material of width 4 mm.

For the calibration we used a system at a random packing of $\varphi = 0.600$ for $l_{\text{box}} = \{2, 3, 4\}$ cm, shown in Fig. 3. The total path length, l_g , is varied by rotating the rectangular box. The parameters obtained from the calibration measurement are

$$\begin{aligned} M &= 0.195 \pm 0.023 \\ \lambda &= (0.213 \pm 0.003) \text{ cm}^{-1} \\ \mu_0 &= (0.992 \pm 0.004) \text{ cm}^{-1}. \end{aligned}$$

Obviously μ_g is depending on l_g significantly. Neglecting the effect of beam hardening leads to wrong packing fractions.

Using Eq. (10) together with these parameters and averaging in horizontal direction over the area highlighted in Fig. 2(right), we obtain the volume fraction profile shown in Fig. 2(left).

The obtained calibration, $\mu_g(l_g)$, can be used to analyze the gray-scale image shown in Fig. 2 (right) to obtain the volume fraction as a function of height shown in Fig. 2 (left). The small variations of the fitted curve to the measured data points validates the use of equation 5. A quantitative comparison of different fit functions is shown in [Baur et al 2018 - work with Matthias](#). The correction with respect to beam hardening outlined in this paper,

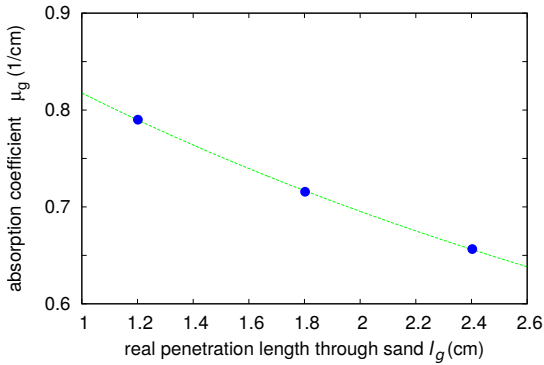


Figure 3: Attenuation coefficient $\mu_g(l_g)$ obtained from the calibration measurements (symbols). The abscissa shows values of $l_g = l_{\text{box}} \varphi$, where $l_{\text{box}} = \{2, 3, 4\}$ cm and $\varphi = 0.6$. The dashed line shows Eq. (5) using the calibrated parameters.

delivers a packing fraction of $\varphi = 0.50$ in the shear band. Since $\mu_g(l_g)$ is far from constant neglecting the effect of beam hardening leads to large deviations from that value (Fig. 3). The full description of the effect of *self-organized migrating shear bands in horizontally shaken granular matter*, including a detailed discussion on the packing density in shear bands, the error analysis and the physical significance of the correction with respect to beam hardening will be given in Ref. (Kollmer et al., 2018).

5. Conclusion

X-ray radiography can be used as an efficient and precise method to determine the spatio-temporal field of density in dynamical granular systems. For quantitative investigations, beam hardening that is the change of the spectral composition of the x-rays passing the object, must be taken into account. In this paper, we describe a protocol for the calibration of the x-ray recordings that relies on measurements of a packing at a single volume fraction which is essential for granular system because it is difficult to prepare a system at a well defined volume fraction. In this *short communication*, we interpolated our data with a simple function to correct beam hardening.

Acknowledgments

The authors thank Dr. Matthias Schröter for enlightening discussion. We acknowledge funding by Deutsche Forschungsgemeinschaft through the Cluster of Excellence “Engineering of Advanced Materials”, ZISC and FPS.

References

- Baxter, G. W., Behringer, R. P., Fagert, T., Johnson, G. A., 1989. Pattern formation in flowing sand. *Phys. Rev. Lett.* 62, 2825–2828.
- Beer, A., 1852. Bestimmung der Absorption des rothen Lichts in farbigen Flüssigkeiten. *Annalen der Physik* 162, 78–88.
- Homan, T., Mudde, R., Lohse, D., van der Meer, D., 2015. High-speed X-ray imaging of a ball impacting on loose sand. *J. Fluid Mech.* 777, 690–706.

- Kabla, A. J., Senden, T. J., 2009. Dilatancy in slow granular flows. *Phys. Rev. Lett.* 102, 228301.
- Kleinschmidt, C., 1999. Analytical considerations of beam hardening in medical accelerator photon spectra. *Medical Physics* 26, 1995–1999.
- Kollmer, J. E., Shreve, T., Claussen, J., Gerth, S., Salamon, M., Uhlmann, N., Schröter, M., Pöschel, T., 2018. Self-organized migrating shear bands in horizontally shaken granular matter. preprint.
- Michalowski, R. L., 1984. Flow of granular material through a plane hopper. *Powder Techn.* 39, 29–40.
- Pöschel, T., Rosenkranz, D. E., 1998. Experimental study of horizontally shaken granular matter — The swelling effect. In: Parisi, J., Müller, S. C., Zimmermann, W. (Eds.), *A Perspective Look at Nonlinear Media: From Physics to Biology and Social Sciences*. Lecture Notes in Physics. Springer, Berlin, Heidelberg, pp. 96–109.
- Pöschel, T., Rosenkranz, D. E., Gallas, J. A. C., 2012. Recurrent inflation and collapse in horizontally shaken granular materials. *Phys. Rev. E* 85, 031307.
- Royer, J. R., Corwin, E. I., Flior, A., Cordero, M.-L., Rivers, M. L., Eng, P. J., Jaeger, H. M., 2005. Formation of granular jets observed by high-speed X-ray radiography. *Nature Phys.* 1, 164–167.
- Yu, M. K., Sloboda, R. S., Murray, B., 1997. Linear accelerator photon beam quality at off-axis points. *Medical Phys.* 24, 233–239.